Electronic Supplementary Information (ESI)

Polypyrrole adorned self-supported, pseudocapacitive zinc vanadium oxide nanoflower and nitrogen-doped reduced graphene oxide based asymmetric supercapacitor device for power density application

Lopamudra Halder, Amit Kumar Das, Anirban Maitra, Aswini Bera, Sarbaranjan Paria, Sumanta Kumar Karan, Suman Kumar Si, Suparna Ojha, Anurima De and Bhanu Bhusan Khatua*

Materials Science Centre, Indian Institute of Technology Kharagpur, Kharagpur-721302, West Bengal, India

*Corresponding Author

Dr. B. B. Khatua (Email: *khatuabb@matsc.iitkgp.ernet.in*).

Materials Science Centre, Indian Institute of Technology, Kharagpur –721302, India.

Tel.:+91-3222-283982

S1. FESEM, TEM analysis, XRD pattern and RAMAN spectroscopic of nitrogen-doped reduced graphene oxide (NG)

The prominent morphological characteristic of typical nitrogen-doped graphene oxide (NG) was found from FESEM analysis (Fig. S1a). The sheets are folded and crumpled in nature resembles to surface of cabbage. Transparent folded sheets were observed from TEM analysis (Fig. S1b). The bubbles within the transparent sheets indicate the doping of nitrogen. Nitrogen doping in reduced graphene oxide promotes the transportation of electrons and hence better capacitive performance. The XRD pattern as obtained from Fig. S1c shows the appearance of diffraction peaks at 25.6° and 43.3° corresponding to the (002) and (100) crystal planes. The smaller and broader peak at 25.6° indicates the exfoliation of graphene oxide and restacking of the layer of GO during the reduction process.[1]

The presence of nitrogen functionality in the reduced graphene oxide has been confirmed by RAMAN analysis. Fig. S1d represents RAMAN spectrum within the range of 800–2000 cm^{-1}. Two prominent peaks appeared at 1349 and 1585 cm^{-1} indicating the presence of D and G band. The D band is associated with defects in graphene sheets and G band is the vibrational frequency of sp^2 hybridized carbon.[2] The greater the intensity ratio of D to G band the greater is the nitrogen doping giving rise to a large number of defects in the material.[3] The calculated I_D/I_G was found to be 1.2 and 0.85 for NG and GO respectively. The increased D/G intensity of NG indicates increased defects and conversion of sp^3 hybridized carbon to sp^2.
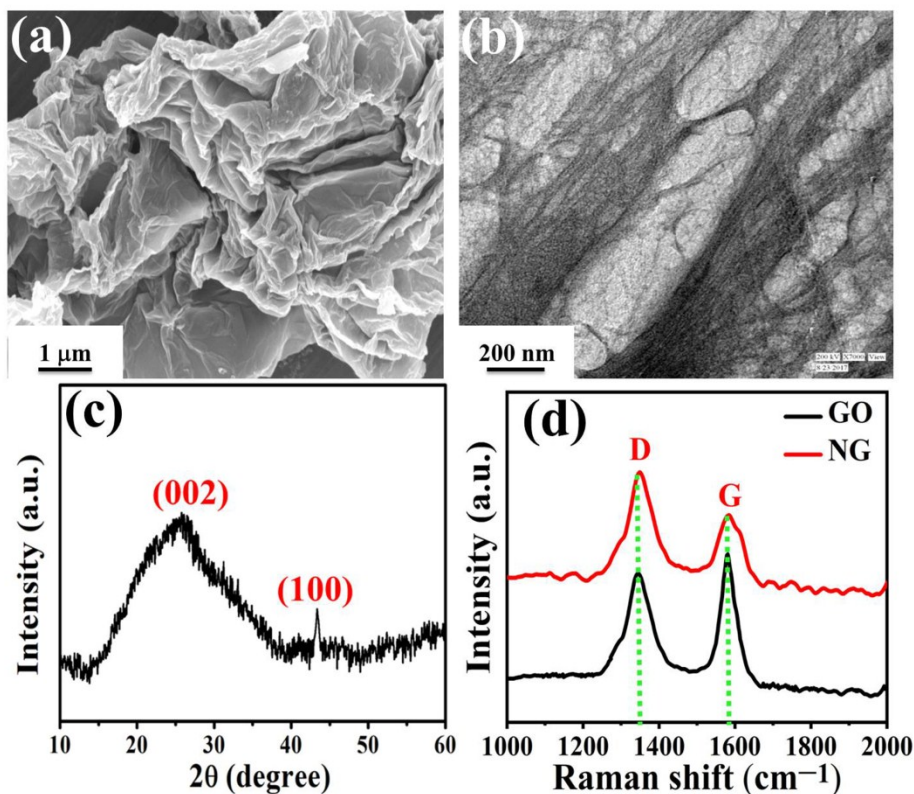
Fig. S1 (a) FESEM micrograph, (b) HRTEM image (c) XRD pattern and, (d) RAMAN 1spectrum of nitrogen-doped reduced graphene NG and GO.

S2. Nitrogen adsorption-desorption isotherm and pore size distribution analysis

The BET specific surface area was obtained from Nitrogen adsorption-desorption isotherm. The pore size distribution was analyzed from the desorption curve following the BJH method. The pore size distribution analysis and the adsorption-desorption isotherm have been represented in Fig. S2. The average pore radius of ZVP and ZV was calculated to be 3.41 and 2.98 nm respectively (as obtained from Fig. S2c, a) signifying the mesoporous nature of the electrode materials. The as-obtained isotherms of the ZV and ZVP resemble with the type– IV hysteresis loop. The overall pore volume of ZV is 0.145 cc g^{-1} at the relative pressure of $(P/P_0) \approx 0.9959$ calculated from the BJH method, with a specific surface area of 36.459 m^2 g^{-1}. Incorporation of PPy in ZVP significantly enhances the specific surface area to 76.054 m^2 g^{-1} and total pore volume was found to be slightly greater i.e. 0.182

cc g^{-1} at (P/P$_0$) ≈ 0.9944 for ZVP. The hysteresis loop in the electrode materials reveals the presence of numerous mesopores in them. However, the hysteresis loop appears due to significant amount of nitrogen gas adsorption on the surface. The gas adsorption widens the hysteresis loop resulting increase in surface area. Therefore, the wider hysteresis loop of ZVP than that of ZV demonstrates the larger surface area of ZVP than ZV. The superior exposed surface area provides additional active sites to initiate electrochemical redox reaction. Additionally, the large numbers of mesopores help to penetrate the electrolyte into the electrode materials resulting in complete wetting of the electrode material and efficient charge transfer and hence results in better electrochemical performance of ZVP.
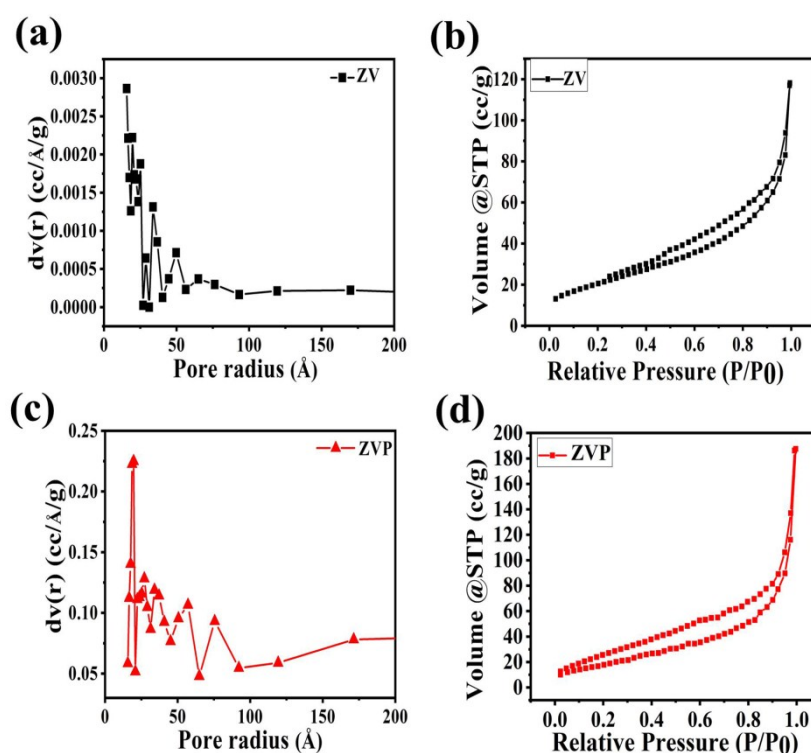
Fig. S2 Pore size distribution analysis and N$_2$ adsorption-desorption isotherm of (a, b) ZV and (c, d) ZVP.

(a)

(b)
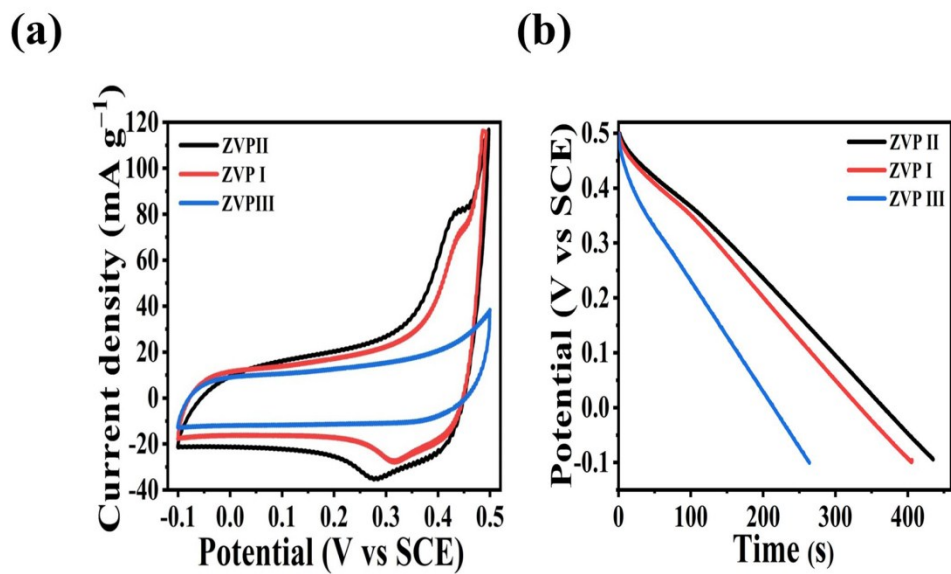
Fig. S3 (a) Comparative CV profiles and (b) GCD plots of ZVP with different weight percent of ZV and PPy.

S3. Charge storage mechanism in electrode materials
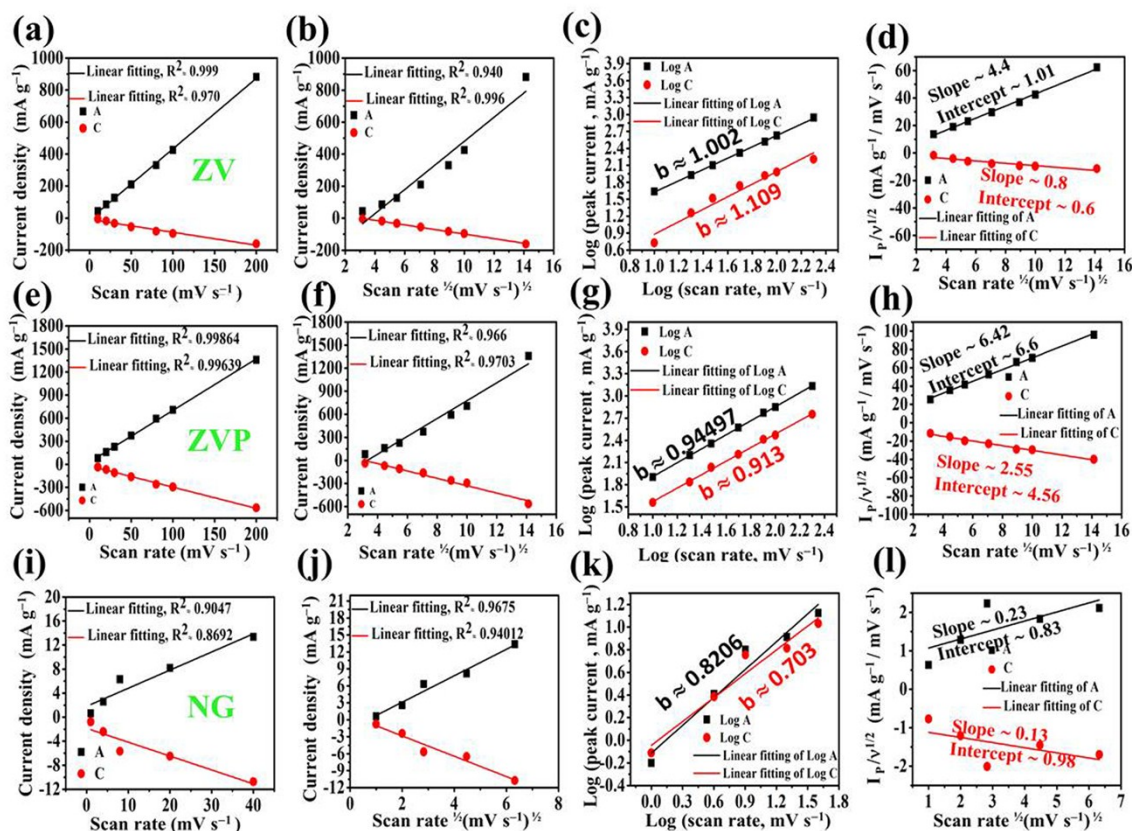
Fig. S4 Kinetic analysis: Variation of anodic and cathodic peak current with scan rates (a) ZV, (e) ZVP, (i) NG. Variation of anodic and cathodic peak current with square root of scan rates (b) ZV, (f) ZVP, (j) NG. Calculation of *b* values from log *i* vs log *ν* plot (c) ZV, (g) ZVP, (k) NG. Plotting $\nu^{1/2}$ vs. I (V)/ $\nu^{1/2}$ to evaluate k_1, k_2 values (d) ZV, (h) ZVP, (l) NG.
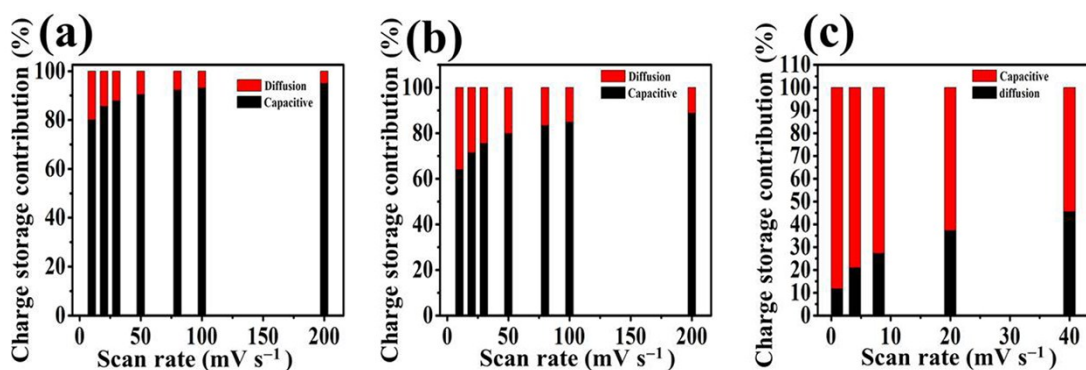
Fig. S5 Capacitive and charge storage contribution at various scan rates of (a) ZV, (b) ZVP, and (c) NG

S4. Electrochemical performance of nitrogen-doped reduced graphene oxide (NG).

Electrochemical performance of nitrogen-doped reduced graphene oxide (NG) coated on stainless steel fabric was evaluated in three-electrode cell setup (where platinum and standard calomel electrode (SCE) were used as counter and reference electrodes respectively) in 1 M KOH electrolyte solution. Before further proceeding to the electrochemical performance, the electrode was charged and discharged for 100 repetitive cycles at 1 A g^{-1} current density to achieve a steady state. The CV profile Fig. S5a demonstrates deviation from the ideal rectangular shape with slight humps at −0.16 V (oxidation peak) and −0.22 V (reduction peak) were observed. The low-intensity redox peaks were appeared due to the presence of nitrogen functionality in reduced graphene oxide, signifying the incorporation of slight pseudocapacitance with EDLC character of reduced graphene oxide. The specific capacitance values were calculated from GCD analysis as represented in Fig. S5b. The C_s values of 587, 563, 494, 419 and 388 F g^{-1} were obtained at 1, 2, 5, 8 and 10 A g^{-1}current densities respectively. The nitrogen doping decreases the active surface area but surprisingly it enhances the specific capacitance remarkably.[4]
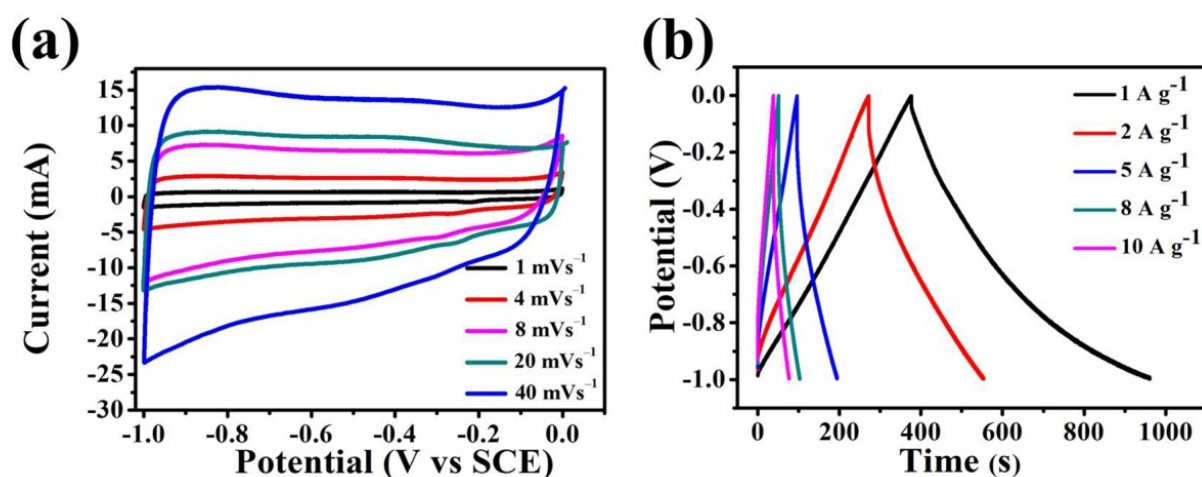
Fig. S6 (a) CV plots and (b) GCD plots of NG.

References

1 J. W. N Lee, J. M. N Ko, J. D. Kim, *Electrochim. Acta*, 2012, **85**, 459–466.

2 Z. Wen, X. Wang, S. Mao, Z. Bo, H. Kim, S. Cui, J. Chen, *Adv. Mater*, 2012, **24**, 5610–5616.

3 K. V. Sankar, R. K. Selvan, R. H. Vignesh, Y. S. Lee, *RSC Adv.*, 2016, **6**, 67898–67909.

4 P. J. Hall, M. Mirzaeian, S. I. Fletcher, F. B. Sillars, A. J. Rennie, G. O. Shitta-Bey, R. Carter, *Energy Environ. Sci.* 2010, **3**, 1238–1251.